DYn-2 Based Identification of *Arabidopsis* Sulfenomes*[S]

Salma Akter[A,B,C,D,E,I], Jingjing Huang[C,D,E], Nandita Bodra[A,B,C,D,E], Barbara De Smet[A,B,C,D,E], Khadija Wahni[C,D,E], Debbie Rombaut[A,B], Jarne Pauwels[F,G], Kris Gevaert[F,G], Kate Carroll[H], Frank Van Breusegem[A,B,J], and Joris Messens[C,D,E,J]

Identifying the sulfenylation state of stressed cells is emerging as a strategic approach for the detection of key reactive oxygen species signaling proteins. Here, we optimized an *in vivo* trapping method for cysteine sulfenic acids in hydrogen peroxide (H_2O_2) stressed plant cells using a dimedone based DYn-2 probe. We demonstrated that DYn-2 specifically detects sulfenylation events in an H_2O_2 dose- and time-dependent way. With mass spectrometry, we identified 226 sulfenylated proteins after H_2O_2 treatment of *Arabidopsis* cells, residing in the cytoplasm (123); plastid (68); mitochondria (14); nucleus (10); endoplasmic reticulum, Golgi and plasma membrane (7) and peroxisomes (4). Of these, 123 sulfenylated proteins have never been reported before to undergo cysteine oxidative post-translational modifications in plants. All in all, with this DYn-2 approach, we have identified new sulfenylated proteins, and gave a first glance on the locations of the sulfenomes of *Arabidopsis thaliana*. *Molecular & Cellular Proteomics 14: 10.1074/mcp.M114.046896, 1183–1200, 2015.*

Among the different amino acids, the sulfur containing amino acids like cysteine are particularly susceptible to oxidation by reactive oxygen species (ROS)[1] (1, 2). Recent studies suggest that the sulfenome, the initial oxidation products of cysteine residues, functions as an intermediate state of redox signaling (3–5). Thus, identifying the sulfenome under oxidative stress is a way to detect potential redox sensors (6, 7).

This central role of the sulfenome in redox signaling provoked chemical biologists to develop strategies for sensitive detection and identification of sulfenylated proteins. The *in situ* trapping of the sulfenome is challenging because of two major factors: (1) the highly reactive, transient nature of sulfenic acids, which might be over-oxidized in excess of ROS, unless immediately protected by disulfide formation (7); (2) the intracellular compartmentalization of the redox state that might be disrupted during extraction procedures, resulting in artificial non-native protein oxidations (8, 9). Having a sulfur oxidation state of zero, sulfenic acids can react as both electrophile and nucleophile, however, direct detection methods are based on the electrophilic character of sulfenic acid (10). In 1974, Allison and coworkers reported a condensation reaction between the electrophilic sulfenic acid and the nucleophile dimedone (5,5-dimethyl-1,3-cyclohexanedione), producing a corresponding thioether derivative (11). This chemistry is highly selective and, since then, has been exploited to detect dimedone modified sulfenic acids using mass spectrometry (12). However, dimedone has limited applications for cellular sulfenome identification because of the lack of a functional group to enrich the dimedone tagged sulfenic acids. Later, dimedone-biotin/fluorophores conjugates have been developed, which allowed sensitive detection and enrichment of sulfenic acid modified proteins (13–15). This approach, however, was not always compatible with *in vivo* cellular sulfenome analysis, because the biotin/fluorophores-conjugated dimedone is membrane impermeable (9) and endogenous biotinylated proteins might appear as false positives.

From the [A]Department of Plant Systems Biology, VIB, 9052 Ghent, Belgium; [B]Department of Plant Biotechnology and Bioinformatics, Ghent University, 9052 Ghent, Belgium; [C]Structural Biology Research Center, VIB, 1050 Brussels, Belgium; [D]Brussels Center for Redox Biology, 1050 Brussels, Belgium; [E]Structural Biology Brussels, Vrije Universiteit Brussel, 1050 Brussels, Belgium; [F]Department of Medical Protein Research, VIB, 9000 Ghent, Belgium; [G]Department of Biochemistry, Ghent University, 9000 Ghent, Belgium; [H]Department of Chemistry, The Scripps Research Institute, Jupiter, FL 33458, USA; [I]Faculty of Biological Sciences, University of Dhaka, 1000 Dhaka, Bangladesh

Received, December 4, 2014 and in revised form, January 19, 2015
Published, MCP Papers in Press, February 18, 2015, DOI 10.1074/mcp.M114.046896
Author contributions: S.A., F.V., and J.M. designed research; S.A., N.B., K.W., D.R., and J.P. performed research; K.G. and K.C. contributed new reagents or analytic tools; S.A., J.H., N.B., B.D., J.P., K.G., F.V., and J.M. analyzed data; S.A., J.H., B.D., F.V., and J.M. wrote the paper.

[1] The abbreviations used are: ROS, reactive oxygen species; IAM, iodoacetamide; MMTS, *S*-methyl methanethiosulfonate; NEM, *N*-ethylmaleimide; SOH, sulfenylation state; S-S, disulfides; SSG, S-glutathionylation; SNO, S-nitrosothiol; H_2O_2, hydrogen peroxide; PTMs, post-translational modifications; c-CRD, carboxy-terminal cysteine-rich domain; PAP, peroxidase-anti-peroxidase; GO, Gene Ontology; YAP1, yeast AP-1 like

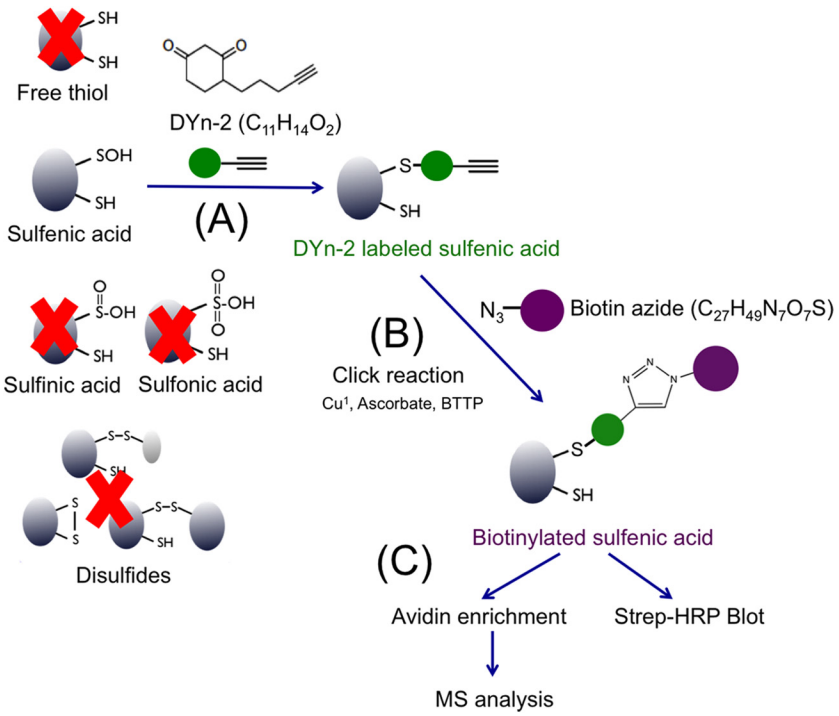

FIG. 1. **Schematic views of the molecular mechanism of the DYn-2 probe and the strategy to identify DYn-2 trapped sulfenylated proteins.** *A*, DYn-2 specifically detects sulfenic acid modifications, but no other thiol modifications. *B*, Biotinylation of the DYn-2 tagged proteins by click reaction. *C*, Once DYn-2 tagged proteins are biotinylated, a streptavidin-HRP (Strep-HRP) blot visualizes sulfenylation, or alternatively, after enrichment on avidin beads, proteins are identified by mass spectrometry analysis.

More recently, the Carroll lab has developed DYn-2, a sulfenic acid specific chemical probe. This chemical probe consists of two functional units: a dimedone scaffold for sulfenic acid recognition and an alkyne chemical handle for enrichment of labeled proteins (9). Once the sulfenic acids are tagged with the DYn-2 probe, they can be biotinylated through click chemistry (16). The click reaction used here is a copper (I)-catalyzed azide-alkyne cycloaddition reaction (17), also known as azide-alkyne Huisgen cycloaddition (16). With this chemistry, a complex is formed between the alkyne functionalized DYn-2 and the azide functionalized biotin. This biotin functional group facilitates downstream detection, enrichment, and mass spectrometry based identification (Fig. 1). In an evaluation experiment, DYn-2 was found to efficiently detect H_2O_2-dependent sulfenic acid modifications in recombinant glutathione peroxidase 3 (Gpx3) of budding yeast (18). Moreover, it was reported that DYn-2 is membrane permeable, non-toxic, and a non-influencer of the intracellular redox balance (17, 18). Therefore, DYn-2 has been suggested as a global sulfenome reader in living cells (17, 18), and has been applied to investigate epidermal growth factor (EGF) mediated protein sulfenylation in a human epidermoid carcinoma A431 cell line and to identify intracellular protein targets of H_2O_2 during cell signaling (17).

Here, we selected the DYn-2 probe to identify the sulfenome in plant cells under oxidative stress. Through a combination of biochemical, immunoblot and mass spectrometry techniques, and TAIR10 database and SUBA3-software predictions, we can claim that DYn-2 is able to detect sulfenic acids on proteins located in different subcellular compartments of plant cells. We identified 226 sulfenylated proteins in response to an H_2O_2 treatment of *Arabidopsis* cell suspensions, of which 123 proteins are new candidates for cysteine oxidative post-translational modification (PTM) events.

EXPERIMENTAL PROCEDURES

Arabidopsis Cell Cultures, Stress Treatments and DYn-2 Labeling—A. thaliana dark grown cell suspension line (PSB-D) was cultured as previously described (19). All experiments were performed with cells in mid-log phase (3-day old, around 10 mg fresh weight/ml). The time and dose of the stress treatment, as well as DYn-2 labeling were performed as follows:

(1) For optimization of DYn-2 labeling conditions, we followed two conditions: (A) 10-ml cell cultures were stressed for 1 h by addition of 0, 0.1, 1 or 20 mM H_2O_2 in separated conical flasks (Merck, Germany). Then, the cells were harvested by filtration and rinsed with culture medium. After resuspension of the stressed cells in culture medium, probe labeling was performed with 0, 0.5, 1, 2.5, 5, or 10 mM of DYn-2 for 1 h. (B) The cell cultures were stressed for 1 h by addition of 0 or 20 mM H_2O_2 in the presence of 5 mM DYn-2. (2) For the detection of the dose-dependent responses of cells to H_2O_2 treatment, 10-ml cell cultures were treated with 0, 0.5, 1, 2, 5, 10, or 20 mM H_2O_2 in the presence of 500 μM DYn-2 for 1 h. For the detection of the time-dependent responses, 50-ml cell cultures were treated with 0, 1, or 20 mM H_2O_2 in the presence of 500 μM DYn-2. After 15, 30, 60, and 120 min treatment, 10 ml of cell culture were harvested at indicated time points for each H_2O_2 concentration. (3) For the competition study with

the YAP1C probe, 10 ml of both *YAP1C* and *YAP1A* overexpressing *Arabidopsis* cell cultures were treated with 0 or 20 mM H_2O_2 for 1 h in the presence of 1 mM DYn-2 probe. For the optimization of DYn-2 labeling, the cells were treated with 20 mM H_2O_2 in the presence of 0, 0.5, 1, 2.5, 5, or 10 mM DYn-2 for 1 h. (4) For mass spectrometry based identification, 20-ml cell cultures were treated with 0 or 10 mM H_2O_2 for 30 min in the presence of 500 μM DYn-2.

After stress treatment and DYn-2 probe labeling, the cells were harvested by filtration and washed 3 times with culture medium, then the cells were ready for protein extraction and click reaction following downstream analysis. Before each experiment, the concentration of H_2O_2 was determined at 240 nm using 43.6 $M^{-1}cm^{-1}$ as the molar extinction coefficient.

Protein Extraction, Click Reaction, Western Blot Analysis—For protein extraction and biotinylation by click reaction, we followed the protocol as previously described (17) with some modifications. It is noteworthy to mention that the use of alkylating agents such as IAM and MMTS is not recommended, as they show reactivity with DYn-2 (unpublished data). Moreover, IAM, NEM, and MMTS are also known to form adducts with Cys-SOH, cleavable under reducing conditions (20). Harvested cells were ground on ice using sand with extraction buffer (25 mM Tris-HCl pH 7.6, 15 mM $MgCl_2$, 150 mM NaCl, 15 mM $pNO_2PhenylPO_4$, 60 mM B-glycerolphosphate, 0.1% Nonidet P-40, 0.1 mM Na_3VO_4, 1 mM NaF, 1 mM phenylmethanesulfonyl fluoride, 1 μM E64, 1× Roche protease inhibitor mixture, 5% ethylene glycol) supplemented with catalase (bovine liver, Sigma-Aldrich, St Louis, MO) at 200 U/ml. The lysates were centrifuged at 16,100 × *g* for 30 min at 4 °C to remove the cell debris. The protein content from the soluble fractions was determined using a standard DC Protein Assay (Bio-Rad Laboratories Inc., Hercules, CA). After removing endogenous biotinylated proteins by NeutrAvidin agarose beads, a click reaction was performed with 100 μg of proteins for 1 h by a rocking incubation at room temperature (17). By incubating for 5 min with 1 mM EDTA, the click reaction was stopped. Protein samples were denatured for 5 min at 96 °C, and then, 25 μg of each protein sample was resolved by SDS-PAGE. Sulfenylation was visualized by immunoblot with 1:80,000 dilution of streptavidin-HRP (Strep-HRP) antibody. Equal loading was confirmed on a Coomassie stained SDS-PAGE gel.

Affinity Enrichment of DYn-2 Tagged Proteins—For liquid chromatography-tandem mass spectrometry (LC-MS/MS) analysis, we performed the click reactions using 1-mg protein fractions after removing endogenous biotinylated proteins by NeutrAvidin agarose beads. Subsequently, the click reactions were stopped and proteins were precipitated in ice-cold acetone containing 10% trichloroacetic acid to remove nonreacted click reagents from the lysates upon incubation overnight at −20 °C. On the second day, the precipitated proteins were pelleted by centrifugation at 16,100 × *g* for 30 min at 4 °C. The pellet was washed twice with ice-cold acetone containing 5 mM dithiotreitol. Then, the pellet was air-dried to remove the acetone from the pellet. After complete resuspension of the precipitated proteins in PBS containing 0.2% SDS, the biotinylated DYn-2 labeled proteins were enriched with 200 μl Neutravidin agarose beads, which had been pre-equilibrated with resuspension buffer. The beads were collected by centrifugation at 2800 × *g* for 2 min, washed with PBS, which was followed by incubation with 5 mM dithiotreitol in the same buffer for 30 min at room temperature. Then, stringent washing steps were performed: 1× PBS, 1 × 1 M NaCl for 5 min, 1x PBS, 1 × 4 M urea for 5 min, 1× PBS, 1× PBS containing 0.2% (w/v) SDS, 3× PBS. After each washing step, the beads were collected by centrifugation as described above. The biotinylated proteins were eluted in 100 μl buffer solution containing 1 mM biotin in 50 mM Tris-HCl, pH 7.1, 1% SDS by boiling for 10 min. The eluted proteins were lyophilized and then resuspended in 15 μl/15 μl H_2O/SDS loading buffer, resolved on SDS-PAGE as a single band (21), and excised for LC-MS/MS analysis.

LC-MS/MS Analysis—The gel bands were washed and subsequently digested in gel with trypsin. The obtained peptide mixtures were analyzed via LC-MS/MS using an Ultimate 3000 RSLC nano LC system (ThermoFisher Scientific, Bremen, Germany), in-line connected to a Q-Exactive mass spectrometer (ThermoFisher Scientific). Here, the peptides were first loaded on a trapping column (made in-house, 100 μm internal diameter (I.D.) × 20 mm, 5 μm beads C18 Reprosil-HD, Dr. Maisch, Ammerbuch-Entringen, Germany). After flushing from the trapping column, the sample was loaded on an analytical column (made in-house, 75 μm I.D. × 150 mm, 5 μm beads C18 Reprosil-HD, Dr. Maisch) packed in a needle (PicoFrit SELF/P PicoTip emitter, PF360-75-15-N-5, New Objective, Woburn, MA). Peptides were loaded with loading solvent (0.1% TFA in water/acetonitrile, 98/2 (v/v)) and separated using a linear gradient from 98% solvent A′ (0.1% formic acid in water) to 40% solvent B′ (0.1% formic acid in water/acetonitrile, 20/80 (v/v)) in 30 min at a flow rate of 300 nL/min. This is followed by a 5-min wash reaching 99% solvent B′. The mass spectrometer was operated in data-dependent, positive ionization mode, automatically switching between MS and MS/MS acquisition for the 10 most abundant peaks in a given MS spectrum. The source voltage was set at 3.4 kV and the capillary temperature was 275 °C. One MS1 scan (*m/z* 400–2000, AGC target 3×10^6 ions, maximum ion injection time 80 ms) acquired at a resolution of 70,000 (at 200 *m/z*) was followed by up to 10 tandem MS scans (resolution 17,500 at 200 m/z) of the most intense ions fulfilling predefined selection criteria (AGC target 5×10^4 ions, maximum ion injection time 60 ms, isolation window 2 Da, fixed first mass 140 *m/z*, spectrum data type: centroid, underfill ratio 2%, intensity threshold $1.7xE^4$, exclusion of unassigned, 1, 5–8, >8 charged precursors, peptide match preferred, exclude isotopes on, dynamic exclusion time 20 s). The HCD collision energy was set to 25% Normalized Collision Energy and the polydimethylcyclosiloxane background ion at 445.120025 Da was used for internal calibration (lock mass).

From the MS/MS data in each LC run, Mascot Generic Files were created using the Distiller software (version 2.4.3.3, Matrix Science, www.matrixscience.com/Distiller). While generating these peak lists, grouping of spectra was allowed in Distiller with a maximal intermediate retention time of 30 s, and a maximum intermediate scan count of five was used where possible. Grouping was done with 0.005 Da precursor tolerances. A peak list was only generated when the MS/MS spectrum contained more than 10 peaks. There was no de-isotoping and the relative signal to noise limit was set at 2. These peak lists were then searched with the Mascot search engine (Matrix Science, London, UK, www.matrixscience.com) using the Mascot Daemon interface (version 2.4, Matrix Science) against the TAIR10 database containing 35,386 protein sequences. The considered variable modifications were DYn-2-cycloaddition, oxidation, dioxidation, and trioxidation of the cysteine residues; oxidation of the methionine residues; pyro-glutamate formation of amino-terminal glutamine residues; and acetylation of the protein N terminus. Mass tolerance on precursor ions was set to 10 ppm (with Mascot's C13 option set to 1), and on fragment ions to 20 mmu. The instrument setting was put on ESI-QUAD. Enzyme was set to trypsin, allowing for one missed cleavage, and cleavage was also allowed when lysine or arginine were followed by proline. Only peptides that were ranked first and scored above the threshold score, set at 99% confidence were withheld. Furthermore, we only included peptides with a minimum length of 8 residues and with a maximum mass deviation from the calculated mass of 2 ppm. The average PSM, peptide and protein FDRs for all analyses were calculated at 0.14%, 0.31% and 0.63% respectively, using the method of Käll *et al.* (22).

We considered the total unique identifications of two independent experimental rounds of the nontreated samples as the background dataset. For the data set of H_2O_2 treated samples, the overlapping identifications of three independent experiments were taken into account. To obtain the H_2O_2-dependent DYn-2 sulfenome, we subtracted the background data sets from the data set of the H_2O_2 treated identifications.

RESULTS AND DISCUSSION

The DYn-2 Probe is an Efficient Approach to Trap and Visualize Sulfenic Acids—For the labeling of sulfenylated proteins in living cells, it is of crucial importance to consider factors that might influence basal levels of cysteine oxidation (17). For *Arabidopsis* cell suspension cultures, these factors could be the changes in physico-chemical parameters of the culture medium, nutrient deficiency, cells grown to the stationary phase, etc. We performed stress treatments with increasing concentrations of H_2O_2 on the 3-day-old PSB-D *Arabidopsis* cell suspension cultures in the presence of DYn-2 (Fig. 3 and supplemental Fig. S1*A*, 1*B*). After harvesting, cells were washed with culture medium to remove excess H_2O_2 and DYn-2. This washing step is necessary to avoid DYn-2 tagging of *de novo* sulfenylated proteins generated during the extraction process. Sample preparation and biotinylation of the DYn-2 tagged proteins with click chemistry were performed as previously described (17), followed by protein separation on SDS-PAGE and visualization of the DYn-2 tagged biotinylated proteins on anti-Strep-HRP Western blots. We observed that DYn-2 is able to penetrate *Arabidopsis* cells and that it could detect sulfenic acids formed under stress. In contrast to mammalian cells (17), we found that the H_2O_2 stress treatment performed in the presence of the DYn-2 probe is an efficient approach to trap and visualize sulfenic acids in *Arabidopsis* cells (Fig. 3 and supplemental Fig. S1). Important to note is that we used a catalase-supplemented extraction buffer to extract soluble protein fractions. Catalase scavenges H_2O_2 that might be generated during the protein extraction procedure; in such a way we control *de novo* sulfenylation during the extraction. A pilot experiment using extraction buffer with and without catalase showed a clear influence of catalase to control post-extraction sulfenic acids formation at higher H_2O_2 concentrations (Fig. 3 and supplemental Fig. S2). By incubating the lysate with NeutrAvidin agarose beads, we removed endogenous biotinylated proteins and the nonsulfenylated proteins sticking to the beads.

DYn-2 Competes with YAP1C Trapping—After optimizing the DYn-2 labeling conditions (H_2O_2 stress treatment in the presence of 500 μM DYn-2 probe (supplemental Fig. S1 and Fig. 3), we assessed whether DYn-2 interaction with sulfenylated proteins quantitatively affects the interaction of the YAP1C genetic probe with sulfenic acids under oxidative stress conditions. YAP1C is the carboxy-terminal, cysteine-rich domain (c-CRD) of the redox-regulated yeast AP-1 like (YAP1) transcription factor that has been adapted to trap protein sulfenic acids *in vivo* (23–25). Briefly, we designed two

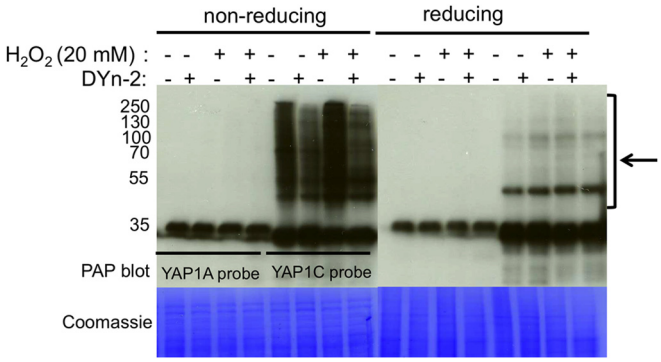

FIG. 2. **The DYn-2 chemical probe competes with the YAP1C genetic probe.** *YAP1C*/*YAP1A* overexpressing cell cultures were treated with 0 or 20 mM H_2O_2 in the presence or absence of DYn-2 for 1 h. Proteins were extracted in the catalase-supplemented extraction buffer, and YAP1C complexes (marked with an arrow) were visualized with the PAP antibody complex. YAP1C complex formation was reduced in the presence of DYn-2 in both nontreated, and H_2O_2 treated *YAP1C-GS* overexpressing *Arabidopsis* cells. Treatment of protein samples with 50 mM TCEP led to the reduction of the YAP1C complexes, indicating the disulfide nature of the complexes.

variants of the YAP1 c-CRD: (1) YAP1C containing the wild-type redox regulatory Cys598 that traps CysSOH residues and (2) YAP1A, in which Cys598 is mutated to alanine as a control for nonspecific protein associations. YAP1 fragments were fused with a GS tag moiety for downstream analysis (26). With the help of a peroxidase-anti-peroxidase (PAP) antibody, which detects the GS tag moiety, we showed that in response to H_2O_2, YAP1C forms mixed disulfides with CysSOH proteins in an H_2O_2 concentration-dependent manner (25). However, these complexes were absent in YAP1A control cells, because the YAP1 c-CRD disulfide-bonded complexes are formed through the specific reaction of Cys598 with CysSOH on multiple proteins.

We performed a competitive study between the DYn-2 and YAP1C probe. Therefore, the *YAP1C* and *YAP1A* overexpressing cells were stressed with 20 mM H_2O_2 for 1 h in the presence or absence of 1 mM DYn-2. As a control, we compared the response with nonstressed cells. Analysis of the Western blots with the PAP antibody showed that the intensity of YAP1C dimerization did not increase in a DYn-2 treated sample under nonstressed conditions (Fig. 2). Further, dimerization bands disappeared under reducing conditions and ran as a monomer with similar levels of YAP1C in each lane, which confirms the redox-active disulfide nature of the interacting proteins. Further, the mixed disulfide complexes were only formed in *YAP1C* overexpressing cells, and were not observed with YAP1A. Under H_2O_2 stressed conditions in the presence of the DYn-2 probe, YAP1C dimerization was decreased (Fig. 2), which indicates that the DYn-2 probe is capable of competing out the reaction with YAP1C, at least for a certain number of sulfenylated proteins (see below and Fig. 4*F*).

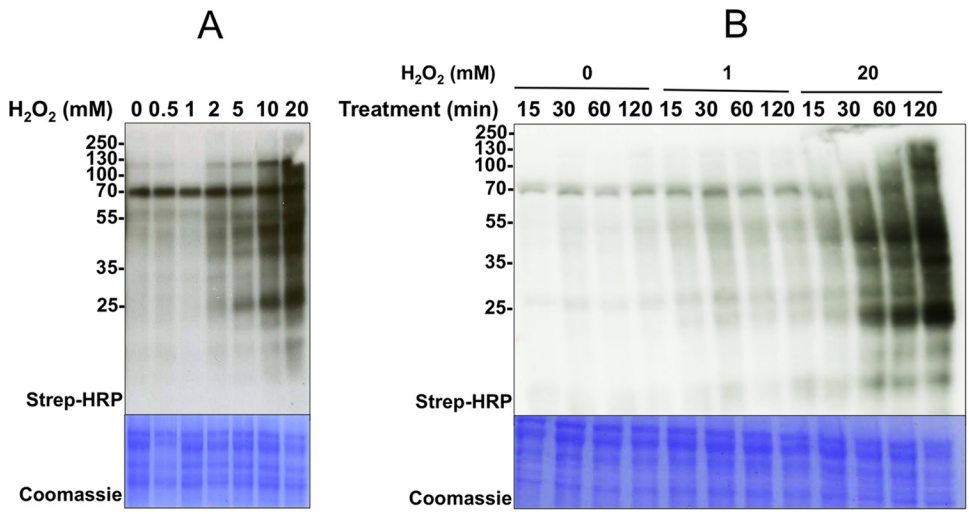

FIG. 3. **DYn-2 detects time- and dose-dependent changes of H_2O_2 mediated sulfenylation in *Arabidopsis*.** *A*, Cell cultures were treated with 0, 0.5, 1, 2, 5, 10, or 20 mM H_2O_2 for 1 h in the presence of 500 μM DYn-2 probe. After the click reaction, the H_2O_2 dose-dependent sulfenylation was visualized on a Strep-HRP developed Western blot. *B*, Cell cultures were treated with 0, 1, or 20 mM H_2O_2 for 15, 30, 60, and 120 min in the presence of 500 μM DYn-2. After the click reaction, the time-dependent sulfenylation was visualized on a Strep-HRP developed Western blot.

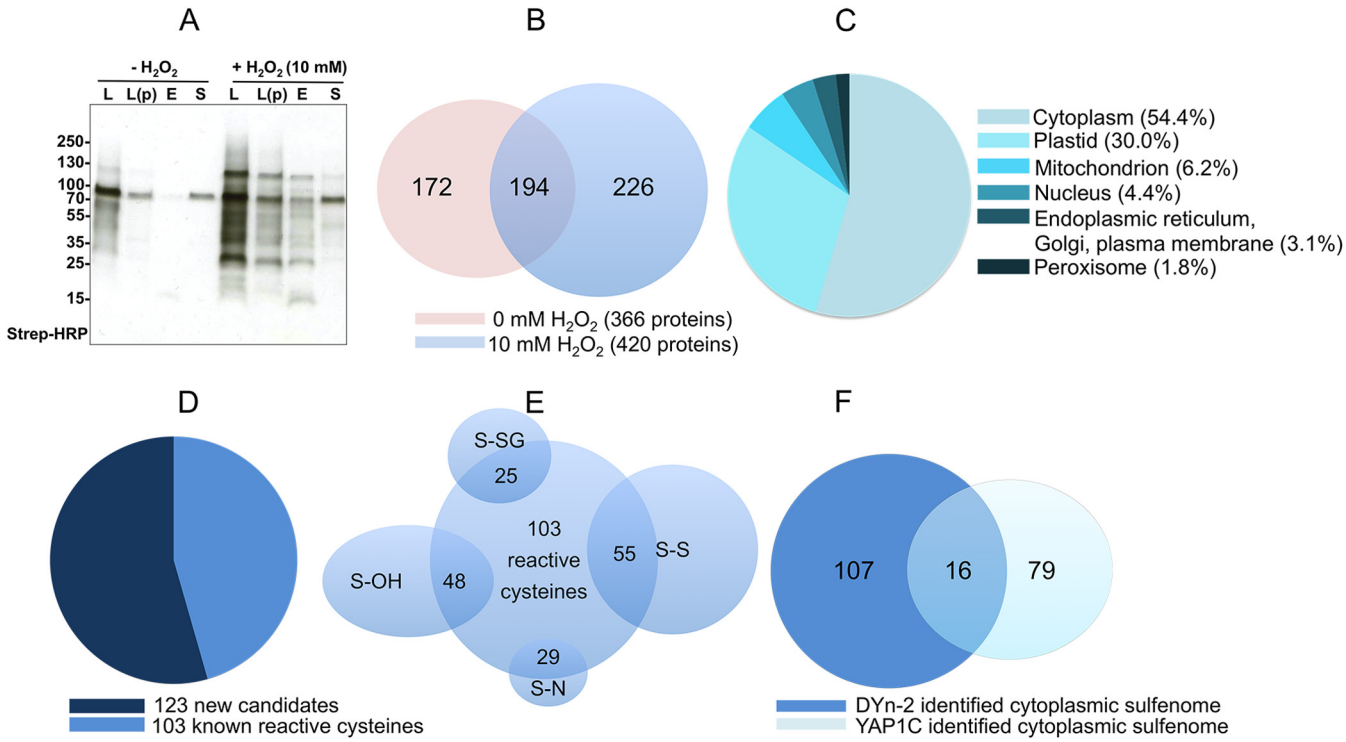

FIG. 4. **Analysis of the sulfenome identified in *Arabidopsis* under H_2O_2 stress.** *A*, Enrichment of DYn-2 tagged proteins. Cell cultures were treated with 0 or 10 mM H_2O_2 for 30 min in the presence of 500 μM DYn-2 probe. After extraction, the DYn-2 tagged proteins were biotinylated and enriched using avidin beads. L: lysates, L(p): Lysates after precipitation, E: eluted proteins, S: Supernatant, the nonbound part of the lysate. On a Strep-HRP developed Western blot, an increased signal was observed under stress conditions even after enrichment of the DYn-2 tagged proteins on avidin beads. *B*, After subtraction of the background datasets of nontreated samples, 226 proteins were identified from three independent experiments as the H_2O_2 mediated DYn-2 sulfenome. *C*, The number of the identified proteins predicted to be present in the different subcellular compartments. *D*, Percentage of the candidates previously identified as having redox-active cysteines. *E*, The previously reported 103 proteins contain sulfenic acids (SOH), disulfides (S-S), S-glutathionylated (SSG), and S-nitrosylated proteins (SNO). *F*, The 123 cytoplasmic sulfenylated proteins identified by DYn-2 contain 16 proteins in common with the YAP1C cytoplasmic sulfenome.

DYn-2 Traps Sulfenylated Proteins under Oxidative Stress in a Time- and Dose-Dependent Manner—After optimizing the DYn-2 labeling conditions, we set out an experiment to optimize the dose of DYn-2 required for sulfenome trapping. We stressed the cells with 20 mM H_2O_2 for 1 h in the absence or presence of increasing concentrations of DYn-2 up to 10 mM. On Strep-HRP Western blot, we observed that DYn-2 is able to detect sulfenic acids at the lowest concentration of 500 μM DYn-2, and that by increasing the DYn-2 concentration, more sulfenylated proteins were detected (supplemental Fig. S3). Because probing at higher concentrations might lead to the presence of nonreacted intracellular DYn-2, we decided to work at the lowest possible concentration of DYn-2. In this way, we lower the possibility of detecting false positive sulfenylation signals, because excess intracellular DYn-2 might tag newly modified proteins during the extraction procedure.

After optimizing the DYn-2 dose for probing sulfenic acids, we set out an experiment to observe whether DYn-2 could detect sulfenylation patterns in a dose-dependent way. Previously, others and we have shown that a 20-mM H_2O_2 treatment of *Arabidopsis* cells provokes cysteine sulfenylation (25, 27). To evaluate the H_2O_2 dose response, we treated the cells with 0, 0.5, 1, 2, 5, 10 or 20 mM H_2O_2 for 1 h in the presence of 500 μM DYn-2 (Fig. 3*A*). On Strep-HRP Western blot, we observed that sulfenic acid labeling by DYn-2 was H_2O_2 dose-dependent. Nonstressed cells displayed only low levels of basal sulfenic acid labeling, whereas an increasing signal was observed from 2 mM of H_2O_2 onward. We concluded that DYn-2 traps the sulfenic acids in a dose-dependent way to H_2O_2 stress responses within the cells.

In the next step, the time course was evaluated. DYn-2 tagging of sulfenic acids was examined for treatment of cell cultures with 0, 1 or 20 mM H_2O_2 and samples were analyzed after 15, 30, 60, and 120 min of each stress treatment (Fig. 3*B*). We observed a response to the changes of sulfenylation in function of time at the 20-mM H_2O_2 treatment. The time-dependent response was not significant at the 1-mM H_2O_2 stressed sample, indicating that this concentration is too low to visualize an increase of the sulfenylation signal. In untreated samples, the intensity of the sulfenylation signal was not changing in function of time, showing that the background oxidation state under nonstressed conditions remains the same in the presence of DYn-2 (Fig. 3*B*). This is an important observation, because it indicates that DYn-2 itself is not generating oxidative stress in *A. thaliana* cells and does not disturb the basal level of sulfenylation under nonstressed conditions. It was also previously reported that DYn-2 does not alter cell viability and glutathione redox balance, or generates ROS in other cell types (18).

Identification of 226 Sulfenylated Proteins under H_2O_2 Stress—As the previous experiments demonstrate that DYn-2 penetrates plant cells and that this small chemical probe (178.2 Da) is able to trap sulfenylated proteins under oxidative stress, we decided to map the sulfenome of *Arabidopsis* cells using this probe. According to the time-course and dose-response experiments, we observed that the sulfenylation signal intensity is similar between the 10- and 20-mM H_2O_2 treatment (Fig 3*A* and supplemental Fig. S2), and we observed a breakthrough of the signal after 30 min of H_2O_2 stress (Fig. 3*B*). Therefore, we decided to stress the *Arabidopsis* cells for 30 min with 10 mM H_2O_2 (Fig. 3*A*) in the presence of 500 μM DYn-2 (breakthrough detection of sulfenylation as observed in supplemental Fig. S3). DYn-2 tagged sulfenylated proteins were extracted and enriched. Before enrichment, the non-reacted click reagents were removed from the lysates by acetone precipitation to avoid competition during the enrichment process between non-clicked free biotin azide and biotinylated DYn-2 tagged proteins. After resuspension of the precipitated protein pellet, DYn-2 tagged proteins were trapped on NeutrAvidin beads. The high affinity of the biotin-avidin interaction (the dissociation constant, K_D, is $\sim 10^{-15}$ M) allowed stringent washing steps (1 M NaCl, 4 M urea) to remove all non-biotinylated interactions. After several intensive, consecutive washing steps (for details see Experimental Procedures), the biotinylated proteins were eluted with biotin competition under denaturing conditions. In Fig. 4*A*, a representative Strep-HRP developed Western blot shows an affinity purification of the DYn-2 tagged proteins of non-stressed and stressed cells. An increased sulfenylation signal in the enriched DYn-2 tagged proteins from stressed cells was observed. Eluted proteins were subjected to LC-MS/MS to identify the sulfenylated proteins. From the three independent experiments of treating cells with 10 mM H_2O_2 for 30 min, we identified 420 different sulfenylated proteins that are present in all rounds. As we wanted to focus on the sulfenylated proteins under H_2O_2 stress, the proteins identified in the absence of H_2O_2 were considered as a background dataset. As such, we identified 226 sulfenylated proteins of the H_2O_2 mediated sulfenome of *A. thaliana* (Fig. 4*B*, supplemental Tables S1 and S2).

DYn-2 Reads the Plant Sulfenome in Different Plant Organelles—We categorized the 226 H_2O_2 mediated sulfenylated proteins based on their predicted or demonstrated subcellular localization, function (Gene Ontology (GO) annotation), and reported cysteine oxidative modifications. Fig. 4*C* displays the predicted subcellular localization of the identified proteins, which suggests the capability of DYn-2 to read the sulfenylation at different subcellular levels *in vivo*. DYn-2 trapped 123 cytoplasmic sulfenylated proteins (54.5%); 68 from the plastids (30%); 10 from the nucleus (4.4%); 14 from mitochondria (6.2%), 7 from the endoplasmic reticulum, Golgi and plasma membrane (3.1%) and 4 from the peroxisome (1.8%) (Table I, Fig. 4*C*). It is noteworthy that we did not perform a specific enrichment for the subcellular proteomes with this approach. The DYn-2 identified proteins have at least one cysteine residue, except for Fe SUPEROXIDE DISMUTASE 1, which might be trapped as a possible interactor of one of the identified proteins (Table I). The majority of the identified proteins are

TABLE I

Overview of the identified sulfenylated candidates with different subcellular localizations in A. thaliana

This table provides the AGI code, description, subcellular localization and functional categorization as provided by the TAIR 10 DB (35 386 protein sequences) and SUBA3. In addition, we provided the number of Cys residues in the corresponding protein sequence and the type of redox modification that was found. Also, references were assigned where possible. These data can be consulted via the PRIDE partner repository with the dataset identifier PXD001562 and 10.6019/PXD001562 (username: reviewer31841@ebi.ac.uk with password: Rg04wyvB) using the PrideInspector tool (48). Details on data validation and search parameters can be found in the Experimental Procedures section. Abbreviations of PTMs are as follows: SNO, S-nitrosothiol; SOH, sulfenic acid; S-S, disulfide bridge; SSG, S-glutathionylation; Trx/Grx target, thioredoxin/glutaredoxin target proteins. References describing identification of homologs/orthologs are marked with an asterisk.

AGI code	Description	Subcellular localization	Functional categorization	No of Cys	Redox modification	References
Cytoplasm						
AT3G62940	OVARIAN TUMOR DOMAIN (OTU)-CONTAINING DUB (DEUBIQUITILATING ENZYME) 5	Cytoplasm, cytosol	Protein degradation	3		
AT2G06990	HEN2, HUA ENHANCER 2	Cytosol, nucleus	RNA binding-translation	14		
AT4G24490	RAB GERANYLGERANYL TRANSFERASE ALPHA SUBUNIT 1	Cytoplasm, cytosol	Protein transport	9		
AT2G45810	DEA(D/H)-box RNA helicase family protein	Cytoplasm, cytosol	RNA binding-translation	10		
AT4G38680	GLYCINE RICH PROTEIN 2, GRP2	Cytoplasm, cytosol	Signal transduction	6		
AT3G29360	UDP-GLUCOSE DEHYDROGENASE 2, UGD2	Cytoplasm, cytosol, nucleus	Primary metabolism	10	SSG	(28)
AT5G63680	Pyruvate kinase family protein	Cytoplasm, cytosol, plasma membrane	Primary metabolism	11		
AT1G62740	HOP2	Cytoplasm, cytosol, nucleus, plasma membrane	Miscellaneous	5	SOH	(25)
AT5G43330	CYTOSOLIC-NAD-DEPENDENT MALATE DEHYDROGENASE 2	Cytoplasm, cytosol, plasma membrane, plasmodesma, apoplast	Primary metabolism	6	Grx target; reactive cys; Trx target	(30*, 49, 50*)
AT2G32520	Alpha/beta-Hydrolases superfamily protein	Cytoplasm, cytosol, chloroplast	Protein degradation	1	Trx target; SNO	(41*, 51*)
AT3G06720	IMPORTIN ALPHA ISOFORM 1	Cytoplasm, cytosol, cell wall, nuclear envelope, nucleolus, nucleus	Protein transport	11		
AT1G69250	Nuclear transport factor 2 (NTF2) family protein with RNA binding (RRM-RBD-RNP motifs) domain	Cytoplasm	RNA binding-translation	3		
AT2G24050	EUKARYOTIC TRANSLATION INITIATION FACTOR ISOFORM 4G2	Cytoplasm, cytosol	RNA binding-translation	10		
AT5G10240	ASPARAGINE SYNTHETASE 3	Cytosol	Amino acid metabolism	12	SOH; reactive cys	(43*, 52)
AT5G49810	METHIONINE S-METHYLTRANSFERASE	Cytoplasm, cytosol	Amino acid metabolism	20		
AT4G13930	SERINE HYDROXYMETHYLTRANSFERASE 4	Cytoplasm, cytosol,	Amino acid metabolism	8	SOH; reactive cys; Trx target; SNO	(41*, 43*, 51*, 52, 53*)
AT3G17820	GLUTAMINE SYNTHETASE 1.3	Cytoplasm, cytosol, cytosolic ribosome, chloroplast	Amino acid metabolism	4	SOH; Trx target	(41*, 43*, 51*)
AT2G05830	5-METHYLTHIORIBOSE KINASE 1	Cytosol, extracellular region, plasmodesma	Amino acid metabolism	4		
AT1G63660	GMP SYNTHASE (glutamine-hydrolyzing)	Cytosol, cytoplasm	Amino acid metabolism	7		
AT3G44310	NITRILASE 1 (NIT1)	Cytosol, apoplast, plasma membrane, plasmodesma	Hormone homeostasis	7	SSG; SOH	(25, 28)
AT1G48630	RECEPTOR FOR ACTIVATED C KINASE 1B (RACK1B)	Cytosol, cytoplasm, cytosolic ribosome, nucleus	Hormone homeostasis	8	SOH; reactive cys	(25, 52)
AT5G09810	ACTIN 7	Cytosol, cytoplasm, cytoskeleton, cell wall	Miscellaneous	4	SSG; SNO; SOH; reactive cys; Trx target	(28, 38, 43*, 49, 50*)

Table I —*continued*

AGI code	Description	Subcellular localization	Functional categorization	No of Cys	Redox modification	References
AT5G44720	Molybdenum cofactor sulfurase family protein	Cytosol, mitochondrion, nucleus, plastid	Miscellaneous and unknown functions	4		
AT5G43830	Aluminium induced protein with YGL and LRDR motifs	Cytosol, nucleus	Miscellaneous and unknown functions	4		
AT4G27450	Aluminium induced protein with YGL and LRDR motifs	Cytosol, nucleus, plasma membrane, plasmodesma	Miscellaneous and unknown functions	7	SOH	(25)
AT4G14930	Survival protein SurE-like phosphatase	Cytosol	Miscellaneous and unknown functions	7		
AT3G22850	Aluminium induced protein with YGL and LRDR motifs	Cytosol, cytoplasm, nucleus, plasma membrane,	Miscellaneous	7		
AT3G13460	EVOLUTIONARILY CONSERVED C-TERMINAL REGION 2	Cytosol, cytoplasm, nucleus	Unknown functions	5		
AT2G15860	Unknown protein	Cytosol, nucleus	Unknown functions	3		
AT1G77550	Tubulin-tyrosine ligases	Cytoplasm, chloroplast	Miscellaneous	14		
AT1G66680	Unknown protein	Cytosol, cytoplasm, nucleus	Miscellaneous	3		
AT1G43690	Ubiquitin interaction motif-containing protein	Cytosol, nucleus	Miscellaneous	12		
AT5G52920	PLASTIDIC PYRUVATE KINASE BETA SUBUNIT 1	Cytosol	Primary metabolism	5		
AT5G48180	NITRILE SPECIFIER PROTEIN 5	Cytosol, cytoplasm	Primary metabolism	7		
AT5G44340	TUBULIN BETA CHAIN 4	Cytosol, cytoplasm, plasma membrane, Golgi, apoplast	Primary metabolism	10	SSG; SNO; SOH	(28, 38, 39, 43*)
AT5G19770	TUBULIN ALPHA-3	Cytosol, cytoplasm, plasma membrane, Golgi, apoplast	Primary metabolism	11	SOH; Trx target	(43*, 50*)
AT5G12250	BETA-6 TUBULIN	Cytosol, cytoplasm	Primary metabolism	12	SOH	(43*)
AT4G37870	PHOSPHOENOLPYRUVATE CARBOXYKINASE 1	Cytosol, cytoplasm, nucleus	Primary metabolism	10		
AT4G16130	ARABINOSE KINASE	Cytosol, cytoplasm, plasmodesma	Primary metabolism	22		
AT4G20890	TUBULIN BETA-9 CHAIN	Cytosol, cytoplasm, plasma membrane, Golgi	Primary metabolism	12	SOH	(43*)
AT3G57890	Tubulin binding cofactor C domain-containing protein	Cytosol, nucleus	Primary metabolism	9		
AT5G58330	NADP-DEPENDENT MALATE DEHYDROGENASE	Cytosol, cytoplasm, apoplast	Primary metabolism	9	Trx target	(32, 33)
AT3G06650	ATP-CITRATE LYASE SUBUNIT B-1	Cytosol, cytoplasm	Primary metabolism	10	SOH	(25)
AT3G06580	GALACTOSE KINASE 1	Cytosol, cytoplasm	Primary metabolism	13		
AT2G41530	S-FORMYLGLUTATHIONE HYDROLASE	Cytosol, cytoplasm, apoplast	Primary metabolism	5	Trx target; reactive cys	(31, 49)
AT1G16350	Aldolase-type TIM barrel family protein	Cytosol	Primary metabolism	6	SSG	(28)
AT1G09780	2,3-BISPHOSPHOGLYCERATE-INDEPENDENT PHOSPHOGLYCERATE MUTASE 1	Cytosol, cytoplasm, apoplast, plasmamembrane	Primary metabolism	4	SNO; Trx target	(39, 50*)
AT1G11840	GLYOXALASE I HOMOLOG	Cytosol, peroxisome, plasmamembrane, chloroplast envelope, mitochondrion	Primary metabolism	1		
AT5G13520	Peptidase M1 family protein	Cytosol, chloroplast	Protein degradation	7	SOH	(25)
AT5G60160	Zn-dependent exopeptidases superfamily protein	Cytosol, chloroplast	Protein degradation	11	Trx target	(31)
AT2G24200	Cytosol aminopeptidase family protein	Cytosol, chloroplast	Protein degradation	5	SSG; SOH; reactive cys; Trx target	(28, 43*, 52)

Table I —*continued*

AGI code	Description	Subcellular localization	Functional categorization	No of Cys	Redox modification	References
AT2G30110	UBIQUITIN-ACTIVATING ENZYME 1	Cytosol, nucleus, plasma membrane	Protein degradation	18		
AT2G19520	MULTICOPY SUPPRESSOR OF IRA1 4	Cytosol, cytoplasm, nucleus	Protein degradation	9		
AT1G22920	COP9 SIGNALOSOME 5A	Cytosol, nucleus	Protein degradation	2	Trx target; SOH	(25, 54)
AT5G22060	DNAJ HOMOLOGUE 2	Cytosol, cytoplasm, plasma membrane	Protein folding	11		
AT4G02450	HSP20-LIKE CHAPERONES SUPERFAMILY PROTEIN	Cytosol, cytoplasm, plasma membrane	Protein folding	1		
AT5G56010	HEAT SHOCK PROTEIN 81–3	Cytosol, cytoplasm, Golgi, plasma membrane	Protein folding	5	SNO; SOH	(38, 43*)
AT5G02500	HEAT SHOCK COGNATE PROTEIN 70–1	Cytosol, cytoplasm, Golgi, plasma membrane	Protein folding	7	SSG; SNO; SOH; Trx target	(28, 39, 43*, 50*, 53*)
AT3G12580	HEAT SHOCK PROTEIN 70	Cytosol, cytosol, plasma membrane	Protein folding	7	SOH; reactive cys; SNO; Trx target	(41*, 42*, 43*, 49, 53*)
AT1G79930	HEAT SHOCK PROTEIN 91	Cytosol, cytosol, plasma membrane	Protein folding	14	Trx target	(53*)
AT1G24510	TCP-1/cpn60 chaperonin family protein	Cytosol, cytosol, plasma membrane, plasmodesma	Protein folding	9	Trx target	(53*)
AT4G34450	Coatomer gamma-2 subunit, putative	Cytosol, Golgi, plasma membrane	Protein transport	12		
AT2G44100	GUANOSINE NUCLEOTIDE DIPHOSPHATE DISSOCIATION INHIBITOR 1	Cytosol, cytoplasm	Protein transport	8		
AT3G14990	DJ-1 HOMOLOG A	Cytosol, plasmamembrane, plasmodesma, nucleus, chloroplast	Redox related	7	SNO; Trx target; reactive cys	(31, 38, 41*, 52)
AT1G78380	GLUTATHIONE S-TRANSFERASE TAU 19	Cytosol, cytoplasm, chloroplast, plasma membrane	Redox related	1	SSG; SNO; Trx target; reactive cys	(28, 31, 32, 38, 55*, 56)
AT1G65980	THIOREDOXIN-DEPENDENT PEROXIDASE 1 (TPX1)	Cytosol, cytoplasm, chloroplast, plasma membrane	Redox related	2	Trx target; reactive cysteine; SNO; SOH; Grx target	(25, 30*, 31, 32, 38, 49)
AT1G60420	ATNRX1, NRX1, NUCLEOREDOXIN 1/DC1 domain-containing protein	Cytosol	Redox related	12	reactive cys	(49)
AT4G14030	SELENIUM-BINDING PROTEIN 1	Cytosol, nucleus	Redox related	7		
AT4G09670	OXIDOREDUCTASE FAMILY PROTEIN	Cytosol	Redox related	6		
AT3G12290	AMINO ACID DEHYDROGENASE FAMILY PROTEIN	Cytosol	Redox related	4		
AT2G21250	NAD(P)-LINKED OXIDOREDUCTASE SUPERFAMILY PROTEIN	Cytosol, cytoplasm	Redox related	6		
AT1G59960	NAD(P)-LINKED OXIDOREDUCTASE SUPERFAMILY PROTEIN	Cytosol, chloroplast	Redox related	5		
AT1G37130	NITRATE REDUCTASE 2	Cytosol, mitochondrion, plasma membrane	Redox related	16	SOH; reactive cys	(25, 52)
AT1G05350	NAD(P)-binding ROSSMANN-fold superfamily protein	Cytosol, cytoplasm	Redox related	10		
AT3G11940	RIBOSOMAL PROTEIN 5A	Cytosol, cytoplasm	RNA binding-translation	2	SNO	(39)
AT3G02760	Class II aaRS and biotin synthetases superfamily protein	Cytosol	RNA binding-translation	17	reactive cys; Trx target	(50*, 52)
AT2G46280	EUKARYOTIC TRANSLATION INITIATION FACTOR 3 SUBUNIT I	Cytosol	RNA binding-translation	5	reactive cys	(52)
AT2G45710	Zinc-binding ribosomal protein family protein	Cytosol	RNA binding-translation	6	reactive cys	(52)
AT1G30580	GTP BINDING /OBG-LIKE ATPASE 1	Cytosol	RNA binding-translation	5	Trx target	(32, 51*)

Table I —*continued*

AGI code	Description	Subcellular localization	Functional categorization	No of Cys	Redox modification	References
AT1G09620	ATP binding*leucine-tRNA ligases*aminoacyl-tRNA ligases*nucleotide binding*ATP binding*aminoacyl-tRNA ligases	cytosol	RNA binding-translation	20	reactive cys	(52)
AT5G25780	EUKARYOTIC TRANSLATION INITIATION FACTOR 3B-2	Cytosol, cytoplasm, nucleus	RNA binding-translation	3		
AT4G39520	GTP-BINDING PROTEIN-RELATED	Cytosol, cytoplasm	RNA binding-translation	7		
AT4G31120	PROTEIN ARGININE METHYLTRANSFERASE 5 (PRMT5)	Cytosol, cytoplasm	RNA binding-translation	12	SOH	(25)
AT4G26870	Class II aminoacyl-tRNA and biotin synthetases superfamily protein	Cytosol, cytoplasm, plasmodesma	RNA binding-translation	11		
AT3G57290	EUKARYOTIC TRANSLATION INITIATION FACTOR 3E (EIF3E)	Cytosol, cytoplasm, plasma membrane	RNA binding-translation	5	SOH	(25)
AT3G04840	Ribosomal protein S3Ae	Cytosol	RNA binding-translation	4		
AT2G40660	Nucleic acid-binding, OB-fold-like protein	Cytosol, cytoplasm, plasmodesma	RNA binding-translation	4		
AT2G40290	Encodes an eIF2alpha homolog	Cytosol	RNA binding-translation	5		
AT2G23350	POLY (A) BINDING PROTEIN 4	Cytosol	RNA binding-translation	7		
AT2G15790	CYCLOPHILIN 40	Cytosol, cytoplasm	RNA binding-translation	7	Trx target	(57*)
AT1G33120	Ribosomal protein L6 family	Cytosol	RNA binding-translation	2		
AT1G10840	TRANSLATION INITIATION FACTOR 3 SUBUNIT H1	Cytosol, cytoplasm	RNA binding-translation	7		
AT3G46940	DUTP-PYROPHOSPHATASE-LIKE 1	Cytosol	Signal perception & transduction	1	reactive cys	(52)
AT5G20990	CO-FACTOR FOR NITRATE REDUCTASE AND XANTHINE DEHYDROGENASE	Cytosol, cytoplasm	Signal perception & transduction	9		
AT5G16050	GENERAL REGULATORY FACTOR 5	Cytosol, cytoplasm, Golgi, plasma membrane	Signal perception & transduction	2		
AT4G24800	EIN2 C-TERMINUS INTERACTING PROTEIN 1	Cytosol	Signal perception & transduction	6		
AT3G15730	PHOSPHOLIPASE D ALPHA 1	Cytosol	Signal perception & transduction	8		
AT3G02870	Encodes a L-galactose-1-phosphate phosphatase, involved in ascorbate biosynthesis.	Cytoplasm, cytosol, plasma membrane	Signal perception & transduction	5		
AT2G43980	INOSITOL 1,3,4-TRISPHOSPHATE 5/6-KINASE 4 (ITPK4)	Cytosol, nucleus	Signal perception & transduction	9	SOH	(25)
AT1G51690	PROTEIN PHOSPHATASE 2A 55KDA REGULATORY SUBUNIT (PP2A-B55A)	Cytoplasm	Signal perception & transduction	11	SOH	(25)
AT1G78300	GENERAL REGULATORY FACTOR 2	Cytosol, cytoplasm, Golgi, plasma membrane	Signal perception & transduction	2	SOH	(43*)
AT1G35160	GENERAL REGULATORY FACTOR 4	Cytosol, cytoplasm, Golgi, plasma membrane	Signal perception & transduction	2	SOH	(43*)
AT5G39570	Unknown protein	Cytosol, nucleus	Unknown functions	1		
AT5G42220	Ubiquitin-like superfamily protein	cytosol, nucleus	Protein degradation	6		
AT5G36210	Alpha/beta-Hydrolases superfamily protein	cytosol, plastid	Protein degradation	13	reactive cys; SOH	(25, 52)
AT4G35830	ACONITASE 1	apoplast, cytoplasm, cytosol, mitochondrion, plasma membrane, plasmodesma, vacuole	Primary metabolism	12	SOH, Trx target	(43*, 50*, 51*)
AT3G53110	LOW EXPRESSION OF OSMOTICALLY RESPONSIVE GENES 4	cytoplasm, nuclear envelope, nucleus, plasma membrane	Miscellaneous and unknown functions	5		

Table I —*continued*

AGI code	Description	Subcellular localization	Functional categorization	No of Cys	Redox modification	References
AT5G19990	REGULATORY PARTICLE TRIPLE-A ATPASE 6A	Cytosol, cytoplasm, nucleus, plasma membrane	Protein degradation	3		
AT1G56450	20S PROTEASOME BETA SUBUNIT G1	Cytosol,	Protein degradation	1	SSG	(28)
AT2G32730	26S PROTEASOME REGULATORY COMPLEX, RPN2	Cytosol, chloroplast	Protein degradation	8		
AT1G20200	EMBRYO DEFECTIVE 2719	Cytosol, nucleus	Protein degradation	6		
AT5G56500	CHAPERONIN-60BETA3	Cytosol, chloroplast	Protein folding	6	Grx target; Trx target	(30*, 53*)
AT3G59020	ARM repeat superfamily protein	Cytosol, cytoplasm, nucleus	Protein transport	16	SOH	(25)
AT3G08943	ARM repeat superfamily protein	Cytosol, cytoplasm	Protein transport	18		
AT3G44300	NITRILASE 2 (NIT2)	Cytosol, plasma membrane	Hormone homeostasis	7	SOH; reactive cys	(25, 49)
AT4G34230	CINNAMYL ALCOHOL DEHYDROGENASE 5	Cytosol, cytoplasm	Primary metabolism	11	Trx target	(31)
AT1G62380	ACC OXIDASE 2	Cytoplasm, cytosol, endoplasmic reticulum, plasma membrane, plasmodesma, Golgi apparatus, cell wall,	Hormone homeostasis	4	SSG	(28)
AT5G53400	BOB1	Cytosol, cytoplasm	Protein folding	4		
AT5G57870	EUKARYOTIC TRANSLATION INITIATION FACTOR ISOFORM 4G1	Cytoplasm, cytosol, nucleus	RNA binding-translation	7		
AT5G56350	Pyruvate kinase family protein	Cytoplasm, cytosol	Primary metabolism	12		
AT1G11650	RNA-binding (RRM/RBD/RNP motifs) family protein	cytoplasm, nucleus	RNA binding	3	reactive cys	(52)
AT4G26970	ACONITASE 2	Cytosol, mitochondrion	Primary metabolism	10	SOH; Trx target	(43*, 50*)
AT5G07440	GLUTAMATE DEHYDROGENASE 2	Cytoplasm, mitochondrion, vacuolar membrane	Amino acid metabolism	6	Trx target; SNO; S-S	(34, 35, 38, 51*)
Mitochondrion						
AT1G48030	MITOCHONDRIAL LIPOAMIDE DEHYDROGENASE 1	Mitochondrion	Carbohydrate metabolism	5	Trx target; Grx target; reactive cys	(30*, 35, 52)
AT1G24180	IAA-CONJUGATE-RESISTANT 4	Mitochondrion	Primary metabolism	8	SOH; reactive cys	(43*, 52)
AT5G08670	ATP SYNTHASE ALPHA/BETA FAMILY PROTEIN	Mitochondrion	Primary metabolism	3	Trx target; Grx target; SSG; SOH; S-S	(28, 30*, 34, 35, 43*)
AT5G50850	MAB1, MACCI-BOU/TRANSKETOLASE FAMILY PROTEIN/PYRUVATE DEHYDROGENASE E1 COMPONENT SUBUNIT BETA-1, MITOCHONDRIAL	Mitochondrion	Primary metabolism	5	S-S bond; reactive cys; Trx target	(34, 35, 49)
AT5G08300	SUCCINYL-COA LIGASE, ALPHA SUBUNIT	Mitochondrion, cell wall	Primary metabolism	8	Trx target	(35, 51*)
AT1G22840	CYTOCHROME C-1	Mitochondrion, cytosol	Primary metabolism	2		
AT5G37510	NADH-ubiquinone dehydrogenase, mitochondrial,	Mitochondrion	Protein degradation	19	Trx target	(35)
AT3G62530	ARM repeat superfamily protein	Mitochondrion, nucleolus, chloroplast,	Protein transport	3	reactive cys	(49)
AT5G43430	ELECTRON TRANSFER FLAVOPROTEIN BETA	Mitochondrion	Redox related	3		
AT5G14040	MITOCHONDRIAL PHOSPHATE TRANSPORTER 3 (MPT3)	Mitochondrion	Signal perception & transduction	7	Trx target; SOH; SNO; S-S	(34, 35, 39, 43*)
AT3G17240	LIPOAMIDE DEHYDROGENASE 2, mitochondrial	Mitochondrion,	Redox related	5	SNO; SOH; S-S	(34, 39, 40, 43*)
AT1G48920	NUCLEOLIN LIKE 1	Mitochondrion, nucleolus	Protein transport	1		
AT5G14590	ISOCITRATE/ISOPROPYLMALATE DEHYDROGENASE FAMILY PROTEIN	Mitochondrion, plastid	Primary metabolism	6	Grx target; SOH	(30*, 43*)
AT1G74260	PURINE BIOSYNTHESIS 4	Mitochondrion, plastid	Primary metabolism	24	reactive cys	(52)
Nucleus						
AT3G51800	ERBB-3 BINDING PROTEIN 1	Nucleolus, nucleus, plasma membrane	Protein transport	6	SOH; SNO	(25, 39)
AT1G35780	Unknown protein*	Nucleus	Unknown function	2		
AT1G22730	MA3 domain-containing protein	Nucleus	Miscellaneous	10		

Table I —*continued*

AGI code	Description	Subcellular localization	Functional categorization	No of Cys	Redox modification	References
AT3G58510	DEA(D/H)-box RNA helicase family protein	Nucleus, peroxisome, plasma membrane	RNA binding-translation	6		
AT2G22400	S-adenosyl-L-methionine-dependent methyltransferases superfamily protein	Nucleus	RNA binding-translation	14		
AT1G67680	SRP72 RNA-binding domain	Nucleus	RNA binding-translation	7		
AT2G38560	TRANSCRIPT ELONGATION FACTOR IIS	Nucleus	Transcription	11		
AT1G20110	FYVE-DOMAIN PROTEIN 1	nucleus	Miscellaneous	14		
AT1G50570	Calcium-dependent lipid-binding (CaLB domain) family protein	nucleus	Miscellaneous	6		
AT1G45000	AAA-type ATPase family protein	Nucleolus, nucleus, plasma membrane, plasmodesma, cell wall, membrane	Protein degradation	3		
Peroxisome						
AT4G16760	ACYL-COA OXIDASE 1	Peroxisome	Primary metabolism	13		
AT3G24170	GLUTATHIONE-DISULFIDE REDUCTASE	Peroxisome	Redox related	8		
AT2G33150	PEROXISOMAL 3-KETOACYL-COA THIOLASE 3	Peroxisome	Signal perception & transduction	9		
AT2G42520	P-LOOP CONTAINING NUCLEOSIDE TRIPHOSPHATE HYDROLASES SUPERFAMILY PROTEIN	Peroxisome	Transcription	4		
Endoplasmic reticulum/Golgi/ Plasma membrane						
AT5G22770	ALPHA-ADAPTIN	Clathrin adaptor complex, membrane, membrane coat, plasma membrane	Protein transport	15		
AT1G05520	Sec23/Sec24 protein transport family protein	Endoplasmic reticulum, Golgi	Protein transport	20		
AT5G42020	LUMINAL BINDING PROTEIN	Endoplasmic reticulum, endoplasmic reticulum lumen	Protein folding	5	SOH; SNO	(38, 43*)
AT1G56340	CALRETICULIN 1A	Endoplasmic reticulum, plasmodesma, apoplast	Protein degradation	3	SOH; reactive cys	(43*, 49)
AT1G09210	CALRETICULIN 1B	Endoplasmic reticulum, apoplast	Protein degradation	4	SOH	(43*)
AT4G23850	LONG-CHAIN ACYL-COA SYNTHETASE 4/ AMP-DEPENDENT SYNTHETASE AND LIGASE FAMILY PROTEIN	Golgi apparatus, plasma membrane, nucleus	Primary metabolism	13		
AT3G08530	CLATHRIN, HEAVY CHAIN 2	Golgi apparatus, plasma membrane, plasmodesma, clathrin coat of trans-Golgi network vesicle	Protein transport	22		
Plastid						
AT2G43750	ARABIDOPSIS CYSTEINE SYNTHASE 1	Plastid	Amino acid metabolism	5	S-S bond; reactive cys; SOH	(37, 43*, 58)
AT3G59760	O-ACETYLSERINE (THIOL) LYASE ISOFORM C	Chloroplast, chloroplast stroma, mitochondrion	Amino acid metabolism	6	Trx target; SOH; S-S; Grx target	(30*, 32, 34, 35, 43*)
AT5G54770	THIAZOLE BIOSYNTHETIC ENZYME, CHLOROPLAST	Plastid	Primary metabolism	2		
AT5G41670	6-phosphogluconate dehydrogenase family protein	Plastid, mitochondrion	Primary metabolism	6		
AT4G24830	Arginosuccinate synthase family	Plastid	Amino acid metabolism	6	reactive cys; SSG; SOH	(25, 28, 49)
AT4G39980	3-DEOXY-D-ARABINO-HEPTULOSONATE 7-PHOSPHATE SYNTHASE 1, DHS1	Chloroplast, mitochondrion	Amino acid metabolism	9		
AT4G35630	PHOSPHOSERINE AMINOTRANSFERASE	Plastid	Amino acid metabolism	8		

Table I —*continued*

AGI code	Description	Subcellular localization	Functional categorization	No of Cys	Redox modification	References
AT4G32520	SERINE HYDROXYMETHYLTRANSFERASE 3	Plastid	Amino acid metabolism	7	Trx target, SNO	(41*, 51*, 53*)
AT4G29840	THREONINE SYNTHASE	Plastid, cytosol	Amino acid metabolism	11	Trx target	(53*)
AT3G57560	N-ACETYL-L-GLUTAMATE KINASE	Plastid, cytoplasm	Amino acid metabolism	4		
AT3G49680	BRANCHED-CHAIN-AMINO-ACID AMINOTRANSFERASE 3, CHLOROPLASTIC	Plastid	Amino acid metabolism	7		
AT2G45300	5-ENOLPYRUVYLSHIKIMATE-3-PHOSPHATE/ EPSP synthase involved in chorismate biosynthesis	Plastid	Amino acid metabolism	10		
AT2G31810	ACT domain-containing small subunit of acetolactate synthase protein	Plastid	Amino acid metabolism	4		
AT2G29690	ANTHRANILATE SYNTHASE 2	Plastid	Amino acid metabolism	7		
AT2G22250	ASPARTATE AMINOTRANSFERASE	Plastid	Amino acid metabolism	6	Trx target; SNO	(41*, 51*)
AT1G80600	HOPW1–1-INTERACTING 1	Plastid, mitochondrion	Amino acid metabolism	7		
AT1G58080	ATP PHOSPHORIBOSYL TRANSFERASE 1	Plastid, cytoplasm	Amino acid metabolism	6		
AT1G48850	EMBRYO DEFECTIVE 1144, chorismate synthase activity	Plastid, nucleolus	Amino acid metabolism	8		
AT1G29900	CARBAMOYL PHOSPHATE SYNTHETASE B	Plastid, mitochondrion	Amino acid metabolism	21		
AT1G22410	Class-II DAHP synthetase family protein	Plastid	Amino acid metabolism	7		
AT5G16290	VALINE-TOLERANT 1	Plastid, cytosol	Amino acid metabolism	2	reactive cys	(52)
AT3G53580	Diaminopimelate epimerase family protein, Chloroplastic	Plastid	Amino acid metabolism	9	reactive cys	(52)
AT3G23940	Dehydratase family	Plastid	Amino acid metabolism	12	Trx target	(31, 33)
AT4G26300	EMBRYO DEFECTIVE 1027	Plastid, mitochondrion	Miscellaneous and unknown functions	9		
AT1G69740	Encodes a putative 5-aminolevulinate dehydratase involved in chlorophyll biosynthesis.	Plastid	Miscellaneous and unknown functions	8		
AT2G33210	HEAT SHOCK PROTEIN 60–2	Plastid, mitochondrion, plasma membrane	Protein folding	7	Trx target; SSG; SOH; Grx target	(28, 30*, 35, 43*, 53*)
AT3G48000	ALDEHYDE DEHYDROGENASE 2	Chloroplast, mitochondrion	Primary metabolism	7	SOH; Grx target; reactive cys, Trx target, SNO	(30*, 41*, 43*, 49, 50*, 51*)
AT3G48990	ACYL-ACTIVATING ENZYME 3	Chloroplast, chloroplast stroma	Primary metabolism	4	reactive cys	(52)
AT1G35720	ANNEXIN 1	Chloroplast, chloroplast stroma, apoplast, plasmodesma, thylakoid, vacuolar membrane, vacuole	Signal perception & transduction	2	SNO; SSG	(29, 38, 39)
AT5G46290	KETOACYL-ACYL CARRIER 3-PROTEIN SYNTHASE I	Plastid	Primary metabolism	9		
AT5G17530	phosphoglucosamine mutase family protein	Plastid, cytoplasm	Primary metabolism	4		
AT5G16440	ISOPENTENYL-DIPHOSPHATE DELTA-ISOMERASE I, chloroplastic	Plastid, cytoplasm	Primary metabolism	4		
AT4G18440	Plastid, cytoplasm	Plastid, cytoplasm	Primary metabolism	4		
AT3G57610	ADENYLOSUCCINATE SYNTHETASE, CHLOROPLASTIC	Plastid	Primary metabolism	8	Trx target	(53*)
AT3G48730	GLUTAMATE-1-SEMIALDEHYDE 2,1-AMINOMUTASE 2	Plastid	Primary metabolism	6	SNO; Trx target	(41*, 51*, 59*)
AT1G74030	ENOLASE 1, CHLOROPLASTIC	Plastid	Primary metabolism	7	SOH; reactive cys; Trx target	(43*, 49, 50*)
AT3G25860	PLASTID E2 SUBUNIT OF PYRUVATE DECARBOXYLASE	Plastid	Primary metabolism	1		
AT3G21110	PURIN 7	Plastid	Primary metabolism	7		
AT2G43710	SUPPRESSOR OF SA INSENSITIVE 2	Plastid	Primary metabolism	3		
AT4G33030	SULFOQUINOVOSYLDIACYLGLYCEROL 1	Plastid	Primary metabolism	9	SNO	(39)
AT2G35040	AICARFT/IMPCHase bienzyme family protein	Plastid	Primary metabolism	10		

Table I —*continued*

AGI code	Description	Subcellular localization	Functional categorization	No of Cys	Redox modification	References
AT2G02500	HEAT SHOCK COGNATE PROTEIN 70–1	Plastid	Primary metabolism	4		
AT1G80560	ISOPROPYLMALATE DEHYDROGENASE 2	Plastid	Primary metabolism	3		
AT3G22960	PLASTIDIAL PYRUVATE KINASE 1	Plastid	Primary metabolism	9	reactive cys	(52)
AT1G74040	2-ISOPROPYLMALATE SYNTHASE 1	Plastid	Primary metabolism	7		
AT3G12780	PHOSPHOGLYCERATE KINASE 1	Plastid	Primary metabolism	2	Trx target; S-S	(31, 37, 53*)
AT2G21170	PLASTID ISOFORM TRIOSE PHOSPHATE ISOMERASE,	Plastid	Primary metabolism	4	Trx target; Grx target, SNO	(30*, 32, 33, 41*, 50*, 59*)
AT1G43800	STEAROYL-ACYL CARRIER PROTEIN Δ9-DESATURASE6	Plastid	Primary metabolism	4		
AT1G36280	L-Aspartase-like family protein	Plastid	Primary metabolism	3		
AT1G22940	THIAMINE REQUIRING 1	Plastid	Primary metabolism	11		
AT1G63770	Peptidase M1 family protein	Plastid	Protein degradation	11		
AT5G15450	CASEIN LYTIC PROTEINASE B3, Encodes a chloroplast-targeted Hsp101 homologue	Plastid	Protein folding	3		
AT5G49910	CHLOROPLAST HEAT SHOCK PROTEIN 70–2	Plastid	Protein folding	2	Trx target; Grx target; S-S, SNO	(30*, 35, 37, 41*, 50*)
AT3G13470	CHAPERONIN-60BETA2	Plastid	Protein folding	7	S-S; Trx target	(37, 54)
AT5G53480	ARM repeat superfamily protein	Plastid	Protein transport	17		
AT5G50920	HEAT SHOCK PROTEIN 93-V	Plastid	Protein folding	4	S-S; Trx target	(37, 53*)
AT4G08390	STROMAL ASCORBATE PEROXIDASE	Plastid	Redox related	2	Trx target; SNO	(35, 42*, 50*)
AT1G63940	MONODEHYDROASCORBATE REDUCTASE 6	Plastid	Redox related	5	Trx target; S-S	(31, 37)
AT4G16155	DIHYDROLIPOYL DEHYDROGENASES	Plastid	Redox related	9	Trx target	(53*)
AT1G12900	GLYCERALDEHYDE 3-PHOSPHATE DEHYDROGENASE A SUBUNIT 2	Plastid	Redox related	5	Grx target; reactive cys; SNO; Trx target	(30*, 41*, 56, 59*)
AT1G79530	GLYCERALDEHYDE-3-PHOSPHATE DEHYDROGENASE OF PLASTID 1	Plastid	Redox related	3	SOH; Trx target	(43*, 53*, 57*)
AT3G58140	Phenylalanyl-tRNA synthetase class IIc family protein /	Plastid	RNA binding-translation	7		
AT5G65430	GENERAL REGULATORY FACTOR 8	Plastid	Signal perception & transduction	2	Grx target; SNO	(30*, 41*)
AT3G56940	COPPER RESPONSE DEFECT 1	Plastid	Transcription	5		
AT2G17630	PHOSPHOSERINE AMINOTRANSFERASE 2	Plastid	Amino acids metabolism	8		
AT1G80270	PENTATRICOPEPTIDE REPEAT 596	Chloroplast envelope	Miscellaneous and unknown functions	6		
AT5G65620	THIMET METALLOENDOPEPTIDASE 1, TOP1	chloroplast, chloroplast stroma, cytosol	Protein degradation	6	S-S; SNO	(37, 41*)

involved in the primary metabolism of multiple pathways (pentose phosphate pathway, glycolysis, TCA cycle, shikimate, amino acid and fatty acid biosynthesis). In addition, we identified proteins involved in signal perception and transduction, hormone homeostasis, transcription/translation, protein degradation/folding/transport (Table I).

Within the DYn-2 sulfenome (Fig. 4*D*, *E*; Table I), some proteins with reactive cysteines have previously been reported. As such, we analyzed that 25 sulfenylated proteins have been reported to be S-glutathionylated (28–30), 55 proteins with a redox-active disulfide bond (31–37), and 29 proteins for S-nitrosylation (38–42) (Fig. 4*E*; Table I). Apart from that, we identified 30 proteins that are in common with the sulfenome of *Medicago truncatula*, which was analyzed using Bio-DCP1, another dimedone chemistry based probe (43) (Table II). Moreover, we also identified several established antioxidant and signaling proteins like CHLOROPLASTIC GLUTAMATE-CYSTEINE LIGASE, STROMAL ASCORBATE PEROXIDASE, GLUTATHIONE S-TRANSFERASE TAU 19, THIOREDOXIN-DEPENDENT PEROXIDASE 1, MONODEHYDROASCORBATE REDUCTASE 6, ACC OXIDASE 2, NUCLEOREDOXIN 1, ANNEXIN 1 and GLYCERALDEHYDE 3-PHOSPHATE DEHYDROGENASE A.

When we compare lists of proteins discovered with the YAP1C (95 cytoplasmic sulfenylated proteins) (25) and DYn-2 (123; Fig. 4*F*, Table II) probes, only 16 proteins were common. This discrepancy is most likely because of the different mode of action and reactivity of both probes, leading to discrete sensitivities. Dimedone reacts with a sulfenic acid at a rate of 2.7×10^{-2} $M^{-1}s^{-1}$ (44). The DYn-2 probe, however, is doing much better, because its reaction rate with dipeptide-SOH is estimated to be 11 $M^{-1}s^{-1}$ (10). Although the rate constant of YAP1C disulfide formation with target sulfenic acids is not yet known, if we compare it with the rate for the reaction of sulfenic acids with thiols to form a disulfide bond (21.6 $M^{-1}s^{-1}$) (10, 44), the YAP1C probe should be more efficient in trapping sulfenic acids compared with DYn-2. Although the dimedone based probe has a modest reaction rate with sulfenic acids, we observed that DYn-2 is able to trap sulfenylated proteins more specifically *in vivo* than YAP1C (Fig. 2). Noteworthy, whether a reaction will occur does not only depend on the reaction rate, but also on the local concentration. Apart from that, YAP1C makes complexes with sulfenic acids through protein–protein interactions, whereas the relatively small DYn-2 molecule directly reacts with the exposed sulfenic acids independently of the local protein conformation. In this way, the chance that DYn-2 is trapped within protein structural cavities will be larger than that for YAP1C. Also, DYn-2 forms a stable covalent bond with the targeted sulfur, whereas the disulfide nature of the YAP1C-target interaction is reversible and these mixed disulfides can be reduced by the cellular reduction system, leading to an underestimation of the number of sulfenylated proteins. All these reasons might account for the relatively modest number of cytoplasmic proteins identified in our previous study (25).

Significance—We report here the first successful application of the DYn-2 chemical probe for the identification of sulfenomes in plants. With an optimized DYn-2 trapping technique, we identified sulfenylated proteins predicted to be cytoplasmic, plastidal, mitochondrial, nuclear, peroxisomal, or residing in the endoplasmic reticulum, Golgi and plasma membrane. Besides the identification of these sulfenomes, our efforts contribute to a more complete view of the cytoplasmic sulfenome with the identification of 107 new cytoplasmic candidates, so we doubled the identified sulfenylated proteins from the cytoplasm.

Although we are making progress, we are still at the discovery phase. With the application of complementary sulfenic acid trapping techniques, the identification of additional proteins of the sulfenome does not inform us about the mechanism behind triggering oxidative stress defense signaling through sulfenylation. We are also trapping proteins in which the cysteine is damaged by oxidation, and which are prone to degradation within the cellular proteasome, or enzymes in which the formation of a sulfenic acid is part of their catalytic cycle. There is certainly room for improvement toward specificity. Future progress in understanding sulfur oxygen switches within the cell strongly depends on the chemical tools and on the technological advances that will be made in the development of new methodologies. Recent promising results have been reported. Yang *et al.* (45) detected about 1000 sulfenylation sites on more than 700 proteins in human cells using a photocleavable biotin linker on a clickable chemical dimedone probe, even though no specificity toward signaling proteins has been built in. In signaling proteins, sulfenic acids are transiently formed. Therefore, it is important to develop chemical probes with a high reaction rate to trap these transiently formed sulfenic acids. Poole *et al.* (46) have shown in their recent work that strained cycloalkynes react with sulfenic acids to yield a stable alkenyl sulfoxide with a reaction rate that is 100 times faster than that of most dimedone based 1,3 dicarbonyl reagents. However, on the other hand, a relatively slower dimedone based probe might facilitate selectivity toward specific stabilized sulfenic acids, which are more likely to be present in signaling pathways than on catalytically regulated active sites. The kinetics of a probe is one issue, but many other challenges lie still ahead before we get a clear view on the regulation of cellular networks driven by oxidative thiol modifications. Progress in this thiol based signaling field will dependent on combining selective chemical probes and new enrichment strategies with the latest omics technologies.

Although we are fully aware of the current technical limitations and the highly dynamic character of oxidative thiol based signaling, we strongly believe that by reading the DYn-2 sulfenome of *A. thaliana*, an additional important piece within the cellular sulfenome jigsaw puzzle is given. On the

TABLE II

List containing 48 previously identified sulfenylated proteins in Medicago truncatula (42). This table provides the AGI code and description from the TAIR 10 DB with the according references. References describing identifications in plants are marked with an asterisk.

AGI code	Description	References
Signal perception and transduction		
AT2G43980	INOSITOL 1,3,4-TRISPHOSPHATE 5/6-KINASE 4 (ITPK4)	(25)
AT1G51690	PROTEIN PHOSPHATASE 2A 55 KDA REGULATORY SUBUNIT B ALPHA ISOFORM (PP2A-b55α)	
AT5G14040	MITOCHONDRIAL PHOSPHATE TRANSPORTER 3 (MPT3)	(43*)
AT1G78300	14–3-3 PROTEIN, GENERAL REGULATORY FACTOR 2	
AT1G35160	14–3-3 PROTEIN, GENERAL REGULATORY FACTOR 4	
Redox related		
AT1G65980	THIOREDOXIN-DEPENDENT PEROXIDASE 1	(25)
AT1G37130	NITRATE REDUCTASE 2	
AT3G17240	LIPOAMIDE DEHYDROGENASE 2, mitochondrial	(43*)
AT1G79530	GLYCERALDEHYDE-3-PHOSPHATE DEHYDROGENASE OF PLASTID 1 (GAPCP-1)	
Protein synthesis, folding, transport		
AT4G31120	PROTEIN ARGININE METHYLTRANSFERASE 5 (PRMT5)	(25)
AT3G57290	EUKARYOTIC TRANSLATION INITIATION FACTOR 3E (EIF3E)	
AT3G59020	ARM repeat superfamily protein	
AT3G51800	ERBB-3 BINDING PROTEIN 1 (EBP1)	
AT5G56010	HEAT SHOCK PROTEIN 81–3	(43*)
AT5G42020	LUMINAL BINDING PROTEIN	
AT5G02500	HEAT SHOCK COGNATE PROTEIN 70–1	
AT3G12580	HEAT SHOCK PROTEIN 70	
AT2G33210	HEAT SHOCK PROTEIN 60–2	
Protein degradation		
AT5G36210	Alpha/beta-Hydrolases superfamily protein	(25)
AT5G13520	Peptidase M1 family protein	
AT1G22920	COP9 SIGNALOSOME 5A (CSN5A)	
AT2G24200	Cytosol aminopeptidase family protein	(43*)
AT1G09210	CALRETICULIN 1B	
AT1G56340	CALRETICULIN 1A	
Primary metabolism		
AT3G06650	ATP-CITRATE LYASE SUBUNIT B-1	(25)
AT4G24830	Arginosuccinate synthase family	
AT3G48000	ALDEHYDE DEHYDROGENASE 2	(43*)
AT1G24180	IAA-CONJUGATE-RESISTANT 4,	
AT5G44340	TUBULIN BETA CHAIN 4	
AT5G19770	TUBULIN ALPHA-3	
AT5G14590	Isocitrate/isopropylmalate dehydrogenase family protein	
AT5G12250	BETA-6 TUBULIN (TUB6)	
AT5G08670	Encodes the mitochondrial ATP synthase beta-subunit	
AT4G35830	ACONITASE 1	
AT4G13930	SERINE HYDROXYMETHYLTRANSFERASE 4	
AT3G59760	O-ACETYLSERINE (THIOL) LYASE ISOFORM C	
AT2G43750	O-ACETYLSERINE (THIOL) LYASE B	
AT3G17820	GLUTAMINE SYNTHETASE 1.3	
AT5G10240	ASPARAGINE SYNTHETASE 3	
AT4G26970	ACONITASE 2	
AT4G20890	TUBULIN BETA-9 CHAIN	
AT1G74030	ENOLASE 1, CHLOROPLASTIC	
Hormone homeostasis		
AT3G44310	NITRILASE 1 (NIT1)	(25)
AT3G44300	NITRILASE 2 (NIT2)	
AT1G48630	RECEPTOR FOR ACTIVATED C KINASE 1B (RACK1B)	
Miscellaneous		
AT4G27450	Aluminium induced protein with YGL and LRDR motifs	(25)
AT1G62740	HOP2, Encodes one of the 36 carboxylate clamp (CC)-tetratricopeptide repeat (TPR) proteins	
AT5G09810	ACTIN 7	(43*)

long run, it will contribute to the unraveling of signaling events along the sulfenome of plants, and it will help our understanding of signaling transduction pathways under oxidative stress in general.

Acknowledgments—We thank Thu H. Truong, Francisco J Garcia, Pablo Martínez-Acedo and Mauro Lo Conte for their excellent technical assistance and training of S.A. We would like to thank Annick Bleys for help in preparing the manuscript.

* This work has been funded by J.M.'s VUB grant (HOA 22), the Research Foundation Flanders (FWO project grants of F.V.B. and J.M.: G0D7914N "Sulfenomics: oxidatieve schakelaars in planten. Hoe zwavelhoudende planteneiwitten via 'agressieve' zuurstof praten"), and K.C. NIH funding sources: GM102187 and CA174986. B.D.S. thanks IWT for a PhD fellowship, and S.A. thanks the Erasmus Mundus External Cooperation Window for a predoctoral fellowship. Further support came from the Ghent University (Multidisciplinary Research Partnership "Biotechnology for a Sustainable Economy," Grant 01MRB510W) and the Interuniversity Attraction Poles Program (IUAP P7/29 "MARS") initiated by the Belgian Science Police Office.

[S] This article contains supplemental Figs. S1 to S3 and Tables S1 and S2.

[J] To whom correspondence should be addressed: Frank Van Breusegem, Department Plant Systems Biology, VIB - Ghent University, Technologiepark 927, B-9052 Gent, Belgium. Tel.: +32 9 331 39 20; Fax: +32 9 331 38 09; E-mail: frank.vanbreusegem@psb.vib-ugent.be; Joris Messens, Structural Biology Research Center, VIB - Vrije Universiteit Brussel. Pleinlaan 2, B-1050 Brussel, Belgium, Tel.: +32 2 6291992; Fax: +32 2 6291963; E-mail: joris.messens@vib-vub.be.

REFERENCES

1. Di Simplicio, P., Franconi, F., Frosalí, S., and Di Giuseppe, D. (2003) Thiolation and nitrosation of cysteines in biological fluids and cells. *Amino Acids* **25,** 323–339
2. Jacques, S., Ghesquière, B., Van Breusegem, F., and Gevaert, K. (2013) Plant proteins under oxidative attack. *Proteomics* **13,** 932–940
3. Delaunay, A., Pflieger, D., Barrault, M.-B., Vinh, J., and Toledano, M. B. (2002) A thiol peroxidase is an H_2O_2 receptor and redox-transducer in gene activation. *Cell* **111,** 471–481
4. Tachibana, T., Okazaki, S., Murayama, A., Naganuma, A., Nomoto, A., and Kuge, S. (2009) A major peroxiredoxin-induced activation of Yap1 transcription factor is mediated by reduction-sensitive disulfide bonds and reveals a low level of transcriptional activation. *J. Biol. Chem.* **284,** 4464–4472
5. Chiang, S. M., and Schellhorn, H. E. (2012) Regulators of oxidative stress response genes in *Escherichia coli* and their functional conservation in bacteria. *Arch. Biochem. Biophys.* **525,** 161–169
6. Leonard, S. E., Reddie, K. G., and Carroll, K. S. (2009) Mining the thiol proteome for sulfenic acid modifications reveals new targets for oxidation in cells. *Acs. Chem. Biol.* **4,** 783–799
7. Roos, G., and Messens, J. (2011) Protein sulfenic acid formation: from cellular damage to redox regulation. *Free Radic. Biol. Med.* **51,** 314–326
8. Go, Y.-M., and Jones, D. P. (2008) Redox compartmentalization in eukaryotic cells. *Biochim. Biophys. Acta* **1780,** 1273–1290
9. Leonard, S. E., and Carroll, K. S. (2011) Chemical "omics" approaches for understanding protein cysteine oxidation in biology. *Curr. Opin. Chem. Biol.* **15,** 88–102
10. Gupta, V., and Carroll, K. S. (2014) Sulfenic acid chemistry, detection, and cellular lifetime. *Biochim. Biophys. Acta* **1840,** 847–875
11. Benitez, L. V., and Allison, W. S. (1974) The inactivation of the acyl phosphatase activity catalyzed by the sulfenic acid form of glyceraldehyde 3-phosphate dehydrogenase by dimedone and olefins. *J. Biol. Chem.* **249,** 6234–6243
12. Carballal, S., Radi, R., Kirk, M. C., Barnes, S., Freeman, B. A., and Alvarez, B. (2003) Sulfenic acid formation in human serum albumin by hydrogen peroxide and peroxynitrite. *Biochemistry* **42,** 9906–9914
13. Poole, L. B., Klomsiri, C., Knaggs, S. A., Furdui, C. M., Nelson, K. J., Thomas, M. J., Fetrow, J. S., Daniel, L. W., and King, S. B. (2007) Fluorescent and affinity-based tools to detect cysteine sulfenic acid formation in proteins. *Bioconjugate Chem.* **18,** 2004–2017
14. Poole, L. B., Zeng, B.-B., Knaggs, S. A., Yakubu, M., and King, S. B. (2005) Synthesis of chemical probes to map sulfenic acid modifications on proteins. *Bioconjugate Chem.* **16,** 1624–1628
15. Charles, R. L., Schröder, E., May, G., Free, P., Gaffney, P. R., Wait, R., Begum, S., Heads, R. J., and Eaton, P. (2007) Protein sulfenation as a redox sensor – proteomics studies using a novel biotinylated dimedone analogue. *Mol. Cell. Proteomics* **6,** 1473–1484
16. Wang, W., Hong, S., Tran, A., Jiang, H., Triano, R., Liu, Y., Chen, X., and Wu, P. (2011) Sulfated ligands for the copper(I)-catalyzed azide-alkyne cycloaddition. *Chem. Asian J.* **6,** 2796–2802
17. Truong, T. H., and Carroll, K. S. (2012) Bioorthogonal chemical reporters for analyzing protein sulfenylation in cells. *Curr. Protoc. Chem. Biol.* **4,** 101–122
18. Paulsen, C. E., Truong, T. H., Garcia, F. J., Homann, A., Gupta, V., Leonard, S. E., and Carroll, K. S. (2012) Peroxide-dependent sulfenylation of the EGFR catalytic site enhances kinase activity. *Nat. Chem. Biol.* **8,** 57–64
19. Van Leene, J., Stals, H., Eeckhout, D., Persiau, G., Van De Slijke, E., Van Isterdael, G., De Clercq, A., Bonnet, E., Laukens, K., Remmerie, N., Henderickx, K., De Vijlder, T., Abdelkrim, A., Pharazyn, A., Van Onckelen, H., Inzé, D., Witters, E., and De Jaeger, G. (2007) A tandem affinity purification-based technology platform to study the cell cycle interactome in *Arabidopsis thaliana*. *Mol. Cell. Proteomics* **6,** 1226–1238
20. Reisz, J. A., Bechtold, E., King, S. B., Poole, L. B., and Furdui, C. M. (2013) Thiol-blocking electrophiles interfere with labeling and detection of protein sulfenic acids. *FEBS J.* **280,** 6150–6161
21. Van Leene, J., Eeckhout, D., Cannoot, B., De Winne, N., Persiau, G., Van De Slijke, E., Vercruysse, L., Dedecker, M., Verkest, A., Vandepoele, K., Martens, L., Witters, E., Gevaert, K., and De Jaeger, G. (2015) An improved toolbox to unravel the plant cellular machinery by tandem affinity purification of *Arabidopsis* protein complexes. *Nat. Protoc.* **10,** 169–187
22. Käll, L., Storey, J. D., MacCoss, M. J., and Noble, W. S. (2008) Posterior error probabilities and false discovery rates: two sides of the same coin. *J. Proteome Res.* **7,** 40–44
23. Takanishi, C. L., and Wood, M. J. (2011) A genetically encoded probe for the identification of proteins that form sulfenic acid in response to H_2O_2 in *Saccharomyces cerevisiae*. *J. Proteome Res.* **10,** 2715–2724
24. Takanishi, C. L., Ma, L.-H., and Wood, M. J. (2007) A genetically encoded probe for cysteine sulfenic acid protein modification *in vivo*. *Biochemistry* **46,** 14725–14732
25. Waszczak, C., Akter, S., Eeckhout, D., Persiau, G., Wahni, K., Bodra, N., Van Molle, I., De Smet, B., Vertommen, D., Gevaert, K., De Jaeger, G., Van Montagu, M., Messens, J., and Van Breusegem, F. (2014) Sulfenome mining in *Arabidopsis thaliana*. *Proc. Natl. Acad. Sci. U.S.A.* **111,** 11545–11550
26. Van Leene, J., Witters, E., Inzé, D., and De Jaeger, G. (2008) Boosting tandem affinity purification of plant protein complexes. *Trends Plant Sci.* **13,** 517–520
27. Desikan, R., A.-H. Mackerness, S., Hancock, J. T., and Neill, S. J. (2001) Regulation of the *Arabidopsis* transcriptome by oxidative stress. *Plant Physiol.* **127,** 159–172
28. Dixon, D. P., Skipsey, M., Grundy, N. M., and Edwards, R. (2005) Stress-induced protein *S*-glutathionylation in *Arabidopsis*. *Plant Physiol.* **138,** 2233–2244
29. Konopka-Postupolska, D., Clark, G., Goch, G., Debski, J., Floras, K., Cantero, A., Fijolek, B., Roux, S., and Hennig, J. (2009) The role of annexin 1 in drought stress in *Arabidopsis*. *Plant Physiol.* **150,** 1394–1410
30. Rouhier, N., Villarejo, A., Srivastava, M., Gelhaye, E., Keech, O., Droux, M., Finkemeier, I., Samuelsson, G., Dietz, K. J., Jacquot, J.-P., and Wingsle, G. (2005) Identification of plant glutaredoxin targets. *Antioxid. Redox Signal.* **7,** 919–929
31. Marchand, C. H., Vanacker, H., Collin, V., Issakidis-Bourguet, E., Le Maréchal, P., and Decottignies, P. (2010) Thioredoxin targets in *Arabidopsis* roots. *Proteomics* **10,** 2418–2428
32. Marchand, C. H., Le Maréchal, P., Meyer, Y., and Decottignies, P. (2006) Comparative proteomic approaches for the isolation of proteins interacting with thioredoxin. *Proteomics* **6,** 6528–6537

33. Marchand, C., Le Maréchal, P., Meyer, Y., Miginiac-Maslow, M., Issakidis-Bourguet, E., and Decottignies, P. (2004) New targets of *Arabidopsis* thioredoxins revealed by proteomic analysis. *Proteomics* **4,** 2696–2706
34. Winger, A. M., Taylor, N. L., Heazlewood, J. L., Day, D. A., and Millar, A. H. (2007) Identification of intra- and intermolecular disulphide bonding in the plant mitochondrial proteome by diagonal gel electrophoresis. *Proteomics* **7,** 4158–4170
35. Yoshida, K., Noguchi, K., Motohashi, K., and Hisabori, T. (2013) Systematic exploration of thioredoxin target proteins in plant mitochondria. *Plant Cell Physiol.* **54,** 875–892
36. Balmer, Y., Vensel, W. H., Tanaka, C. K., Hurkman, W. J., Gelhaye, E., Rouhier, N., Jacquot, J.-P., Manieri, W., Schürmann, P., Droux, M., and Buchanan, B. B. (2004) Thioredoxin links redox to the regulation of fundamental processes of plant mitochondria. *Proc. Natl. Acad. Sci. U.S.A.* **101,** 2642–2647
37. Ströher, E., and Dietz, K. J. (2008) The dynamic thiol-disulphide redox proteome of the *Arabidopsis thaliana* chloroplast as revealed by differential electrophoretic mobility. *Physiol. Plantarum.* **133,** 566–583
38. Lindermayr, C., Saalbach, G., and Durner, J. (2005) Proteomic identification of *S*-nitrosylated proteins in *Arabidopsis*. *Plant Physiol.* **137,** 921–930
39. Fares, A., Rossignol, M., and Peltier, J. B. (2011) Proteomics investigation of endogenous *S*-nitrosylation in *Arabidopsis*. *Biochem. Bioph. Res. Co.* **416,** 331–336
40. Palmieri, M. C., Lindermayr, C., Bauwe, H., Steinhauser, C., and Durner, J. (2010) Regulation of plant glycine decarboxylase by *S*-nitrosylation and glutathionylation. *Plant Physiol.* **152,** 1514–1528
41. Tanou, G., Job, C., Rajjou, L., Arc, E., Belghazi, M., Diamantidis, G., Molassiotis, A., and Job, D. (2009) Proteomics reveals the overlapping roles of hydrogen peroxide and nitric oxide in the acclimation of citrus plants to salinity. *Plant J.* **60,** 795–804
42. Abat, J. K., and Deswal, R. (2009) Differential modulation of *S*-nitrosoproteome of *Brassica juncea* by low temperature: change in *S*-nitrosylation of Rubisco is responsible for the inactivation of its carboxylase activity. *Proteomics* **9,** 4368–4380
43. Oger, E., Marino, D., Guigonis, J.-M., Pauly, N., and Puppo, A. (2012) Sulfenylated proteins in the *Medicago truncatula-Sinorhizobium meliloti* symbiosis. *J. Proteomics* **75,** 4102–4113
44. Paulsen, C. E., and Carroll, K. S. (2013) Cysteine-mediated redox signaling: chemistry, biology, and tools for discovery. *Chem. Rev.* **113,** 4633–4679
45. Yang, J., Gupta, V., Carroll, K. S., and Liebler, D. C. (2014) Site-specific mapping and quantification of protein *S*-sulphenylation in cells. *Nat. Commun.* **5,** 4776
46. Poole, T. H., Reisz, J. A., Zhao, W., Poole, L. B., Furdui, C. M., and King, S. B. (2014) Strained cycloalkynes as new protein sulfenic acid traps. *J. Am. Chem. Soc.* **136,** 6167–6170
47. Vizcaíno, J. A., Deutsch, E. W., Wang, R., Csordas, A., Reisinger, F., Rios, D., Dianes, J. A., Sun, Z., Farrah, T., Bandeira, N., Binz, P.-A., Xenarios, I., Eisenacher, M., Mayer, G., Gatto, L., Campos, A., Chalkley, R. J., Kraus, H.-J., Albar, J. P., Martinez-Bartolome, S., Apweiler, R., Omenn, G. S., Martens, L., Jones, A. R., and Hermjakob, H. (2014) ProteomeXchange provides globally coordinated proteomics data submission and dissemination. *Nat. Biotechnol.* **32,** 223–226
48. Wang, R., Fabregat, A., Ríos, D., Ovelleiro, D., Foster, J. M., Côté, R. G., Griss, J., Csordas, A., Perez-Riverol, Y., Reisinger, F., Hermjakob, H., Martens, L., and Vizcaíno, J. A. (2012) PRIDE Inspector: a tool to visualize and validate MS proteomics data. *Nat. Biotechnol.* **30,** 135–137
49. Wang, H., Wang, S., Lu, Y., Avarez, S., Hicks, L. M., Ge, X., and Xia, Y. (2012) Proteomic analysis of early-responsive redox-sensitive proteins in *Arabidopsis*. *J. Proteome Res.* **11,** 412–424
50. Wong, J. H., Cai, N., Balmer, Y., Tanaka, C. K., Vensel, W. H., Hurkman, W. J., and Buchanan, B. B. (2004) Thioredoxin targets of developing wheat seeds identified by complementary proteomic approaches. *Phytochemistry* **65,** 1629–1640
51. Balmer, Y., Koller, A., Val G. D., Schürmann, P., and Buchanan, B. B. (2004) Proteomics uncovers proteins interacting electrostatically with thioredoxin in chloroplasts. *Photosynth. Res.* **79,** 275–280
52. Liu, P., Zhang, H., Wang, H., and Xia, Y. (2014) Identification of redox-sensitive cysteines in the *Arabidopsis* proteome using OxiTRAQ, a quantitative redox proteomics method. *Proteomics* **14,** 750–762
53. Balmer, Y., Vensel, W. H., Hurkman, W. J., and Buchanan, B. B. (2006) Thioredoxin target proteins in chloroplast thylakoid membranes. *Antioxid. Redox. Sign.* **8,** 1829–1834
54. Yamazaki, D., Motohashi, K., Kasama, T., Hara, Y., and Hisabori, T. (2004) Target proteins of the cytosolic thioredoxins in *Arabidopsis thaliana*. *Plant Cell Physiol.* **45,** 18–27
55. Bykova, N. V., Hoehn, B., Rampitsch, C., Banks, T., Stebbing, J.-A., Fan, T., and Knox, R. (2011) Redox-sensitive proteome and antioxidant strategies in wheat seed dormancy control. *Proteomics* **11,** 865–882
56. Muthuramalingam, M., Matros, A., Scheibe, R., Mock, H. P., and Dietz, K. J. (2013) The hydrogen peroxide-sensitive proteome of the chloroplast *in vitro* and *in vivo*. *Front. Plant Sci.* **4,** 54
57. Motohashi, K., Kondoh, A., Stumpp, M. T., and Hisabori, T. (2001) Comprehensive survey of proteins targeted by chloroplast thioredoxin. *Proc. Natl. Acad. Sci. U.S.A.* **98,** 11224–11229
58. Alvarez, S., Zhu, M., and Chen, S. (2009) Proteomics of *Arabidopsis* redox proteins in response to methyl jasmonate. *J. Proteomics* **73,** 30–40
59. Wong, J. H., Balmer, Y., Cai, N., Tanaka, C. K., Vensel, W. H., Hurkman, W. J., and Buchanan, B. B. (2003) Unraveling thioredoxin-linked metabolic processes of cereal starchy endosperm using proteomics. *FEBS Lett.* **547,** 151–156